Electrochemical reactions on catalyst particles with three-phase boundaries

V. P. Zhdanov*
Department of Applied Physics, Chalmers University of Technology, S-41296 Göteborg, Sweden
and Boreskov Institute of Catalysis, Russian Academy of Sciences, Novosibirsk 630090, Russia
(Received 26 August 2002; published 10 April 2003)

In fuel cells, electrochemical reactions are often assumed to occur on metal catalyst particles contacting simultaneously the ion-conducting electrolyte and gas phase. Our kinetic Monte Carlo simulations demonstrate that in this case the deviations from the Tafel law in the dependence of the reaction rate on the electrode potential may be related to diffusion of one of the adsorbed reactants along catalyst particles.

DOI: 10.1103/PhysRevE.67.0426XX PACS number(s): 82.45.Fk, 05.60.Cd, 81.07.Bc, 82.45.Jn

Electrochemistry is an old interdisciplinary science attracting attention of physicists and chemists already several centuries [1]. In the past, electrochemical reactions (ECR) were experimentally studied primarily on polycrystalline electrodes. Recent academic investigations in this field are focused on ECR running on single-crystal electrodes [2]. In applications, e.g., in fuel cells [1,3], ECR often occur on nanometer-sized ($\sim$10 nm) metal particles, deposited on the walls of pores of a more or less inactive conducting support, or on metal grains forming a porous network. Despite the long-standing interest, the understanding of mechanisms and kinetics of ECR is still limited, because the common surface-science techniques are often difficult to apply on the electrolyte-metal interface (especially in the case of porous electrodes), and have not by far provided the same wealth of knowledge as gas-solid interfacial studies.

The progress in experimental investigations of ECR is, however, rapid (the most recent advances include, e.g., the use of model planar supported catalysts [4]). The corresponding theoretical studies are focused primarily on ECR running on single-crystal surfaces [5]. There are also several treatments of the kinetics of ECR occurring in fuel cells [6]. The latter works employing the conventional chemical-engineering approaches are aimed at describing the global kinetics, including the interplay of reactant diffusion in the electrolyte and/or gas phase and chemical conversion on catalyst particles. As a rule, the elementary reaction steps are not analyzed there in detail. Instead, the ECR rate is simply assumed to be proportional to local reactant concentration. Rare theoretical studies including reaction steps on metal particles (see, e.g., recent interesting works [7,8]) are based on the simplest mean-field (MF) equations ignoring the specifics of nm chemistry (e.g., the difference of the energetics of reactant adsorption on various interfaces). In this paper we present the first Monte Carlo (MC) simulations of the kinetics of ECR occurring on metal catalyst particles. Our goal is to scrutinize the reaction regimes which can hardly be treated by using the MF approximation.

The specific catalytic activity (i.e., the activity of an adsorption site) of metal particles may be quite different compared to that of macroscopic single-crystal samples. This *structure gap* can be associated with several factors such as unique electronic properties of metal particles, contribution of special sites (e.g., edges) to the reaction rate, metal-support interaction [9], and/or with purely kinetic effects, such as the interplay of the reaction kinetics running on different communicating facets [10]. In electrochemistry, the structure gap may also be related to the specific factors. In particular, the most advanced fuel cells contain metal particles exhibiting so-called *three-phase boundaries* [1,3,7]. Practically, this means that metal particles are in contact simultaneously with the ion-conducting electrolyte and gas phase, supplying one and another reactant, respectively (see the insets in Fig. 1). The unique feature of such systems is that reaction includes reactant transport between phase boundaries. Below, we treat the kinetics of the generic $A+B\rightarrow AB$ reaction occurring on metal particles with three-phase boundaries.

In our model, irreversible adsorption of A^- ions, $A^-_{\rm el}\rightarrow A_{\rm ads}+e$, occurs on the electrolyte-metal boundary. Reversible B adsorption, $B_{\rm gas}\rightleftharpoons B_{\rm ads}$, runs on the gas-metal interface. Adsorbed A species are allowed to diffuse to the gas-metal boundary and to react there with B particles, $A_{\rm ads}+B_{\rm ads}\rightarrow AB_{\rm gas}$. Adsorbed B particles migrate only on the gas-metal boundary. [These steps mimic, e.g., the performance of the H_2-O_2 solid-oxide fuel cell anode (Fig. 1). In particular, A^- and B stand for oxygen ions and H_2 molecules. This attribution is qualitatively correct although the charge of oxygen ions is -2 and H_2 adsorption is dissociative.]

In the MF approximation implying rapid interboundary A diffusion, the steady-state kinetics of ECR under consideration is described as

$$\kappa k^A_{\rm ad} c_A(1-\vartheta_A)=(1-\kappa)k_{\rm r}\theta_A\theta_B, \tag{1}$$

$$k^B_{\rm ad}P_B(1-\theta_A-\theta_B)=k^B_{\rm des}\theta_B+k_{\rm r}\theta_A\theta_B, \tag{2}$$

$$\vartheta_A/(1-\vartheta_A)=\exp(\Delta E/k_{\rm B}T)\,\theta_A/(1-\theta_A-\theta_B), \tag{3}$$

where c_A is the A^- concentration in the electrolyte, P_B is the B pressure in the gas phase, ϑ_A, θ_A, and θ_B are the reactant coverages on the electrolyte-metal and gas-metal interfaces, $k^A_{\rm ad}$, $k^B_{\rm ad}$, $k^B_{\rm des}$, and $k_{\rm r}$ are the adsorption, desorption, and reaction rate constants, ΔE is the difference of the A binding energies on the two interfaces ($\Delta E>0$ if the binding energy is higher on the electrolyte-metal interface), and κ and (1

*Electronic address: zhdanov@catalysis.nsk.su

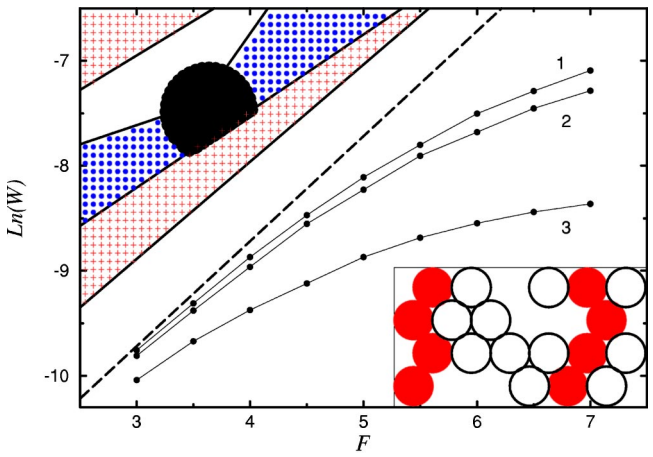

FIG. 1. (Color online) Logarithm of the reaction rate (per MCS) as a function of the normalized electrode potential, $F \equiv \alpha e_0 \varphi_e / k_B T$. Curves (1)–(3) show the MC results in the cases when the A binding energy on the electrolyte-metal interface is lower than $[\exp(\Delta E/k_B T)=0.1]$, equal to $(\Delta E=0)$, and higher than $[\exp(\Delta E/k_B T)=10]$ that on the gas-metal interface (the statistical error is smaller than or comparable to the size of the data points). The dashed curve corresponds to the Tafel law, $W=\kappa(1-\kappa)^{-1}p_0^A \exp(F)$, for the case when the reaction rate is limited by A^- adsorption. [The two insets schematically show typical porous catalysts with three-phase boundaries. In particular, the lower insert represents the structure of a H_2-O_2 solid-oxide fuel cell anode [7] consisting of the metal and solid-oxide grains (e.g., Ni and ZrO_2) which are indicated by filled and open circles. In this case, O^{2-} ions and H_2 molecules are supplied on the catalyst surface via the electrolyte and gas phase, respectively. The upper panel exhibits the electrode structure of H_2-O_2 solid-polymer-electrolyte fuel cells [3]. In the latter case, a Pt or Pt/Ru catalyst particle (large filled circle), located on the carbon support (plus signs), is in contact with the electrolyte (small filled circles).]

$-\kappa$) are the fractions of adsorption sites belonging to the electrolyte-metal and gas-metal interfaces. Equations (1) and (2) describe the balance of A and B species, respectively. Equation (3) indicates that the chemical potentials of A particles on the two interfaces are equal. A^- adsorption is accompanied by electron transfer and accordingly the corresponding rate constant can be represented in the Tafel (or Butler-Volmer) form [11], $k_{ad}^A = k_0 \exp(\alpha e_0 \varphi_e / k_B T)$, where φ_e is the electrode potential, k_0 the potential-independent factor, $\alpha \simeq 0.5$ the so-called transfer coefficient, and e_0 the absolute value of the electron charge. The other rate constants are independent of φ_e.

If the AB-formation step is rapid, the coverages ϑ_A and θ_A are low, the reaction rate is limited by A^- adsorption, and accordingly the reaction rate calculated per adsorption site on the gas-metal interface is given by the Tafel law,

$$W = \kappa(1-\kappa)^{-1} k_0 c_A \exp(\alpha e_0 \varphi_e / k_B T). \quad (4)$$

With increasing rate of A^- adsorption (or decreasing k_r), the MF approximation predicts deviations from the Tafel law. In particular, the reaction rate will be lower than that given by Eq. (4) and the effect of the electrode potential on the ECR kinetics will be weaker.

The MF results are robust provided that adsorbate diffusion is fast. In reality, this is not always the case. If, e.g., A represents oxygen, A diffusion may be relatively slow, because the corresponding activation energy will be appreciable (about or higher than 15 kcal/mol in the case of Pt [12]). Thus, with increasing electrode potential, A^- adsorption may become so rapid that the reaction will be limited by A diffusion from the electrolyte-metal interface to the gas-metal interface. To illustrate the features of such reaction regimes, we employ MC simulations.

To mimic a catalyst particle, we use a 100×100 square lattice with the "no flux" boundary conditions (i.e., the reactants are not allowed to jump over the boundaries). The central 50×50 part of the lattice represents the gas-metal interface, and the periphery corresponds to the electrolyte-metal interface (in reality, the relative areas of the interfaces may be slightly different for different catalyst particles, but for our present analysis this point is not important). A^- and B adsorb, respectively, on the peripheral and central parts of the lattice. The $A_{ads}+B_{ads}$ reaction occurs between reactants located in nearest-neighbor (NN) sites on the central part of the lattice. A and B diffuse via jumps to vacant NN sites. A particles may migrate from the periphery to the center. B particles may move only on the central part of the lattice.

B diffusion is assumed to be much faster compared to the catalytic cycle and A diffusion (such cases are typical in catalytic reactions). To characterize the relative rates of B diffusion and other steps, we use the dimensionless parameter p $(p \ll 1)$. The rates of these processes are considered to be proportional to $(1-p)$ and p, respectively. In addition, we introduce a set of dimensionless probabilities p_{ad}^A, p_{ad}^B, p_{des}^B, p_r, and p_{dif}^A characterizing the rate processes inside the catalytic cycle and A diffusion. As usual in MC simulations, these probabilities can be obtained by normalizing the corresponding rates or rate constants. In our simulations, we analyze the practically interesting case when the B-adsorption rate is equal to or faster than the rates of other steps (except B diffusion). In this case, the rate constants can be normalized to $k_{ad}^B P_B$, i.e., we have $p_{ad}^B = k_{ad}^B P_B / k_{ad}^B P_B \equiv 1$, $p_{des}^B = k_{des}^B / k_{ad}^B P_B$, $p_{ad}^A = k_{ad}^A c_A / k_{ad}^B P_B$, $p_r = k_r / k_{ad}^B P_B$, and $p_{dif}^A = k_{dif}^A / k_{ad}^B P_B$. To take into account that k_{ad}^A depends on φ_e, we represent the A^--adsorption probability as $p_{ad}^A = p_0^A \exp(\alpha e_0 \varphi_e / k_B T)$, where $p_0^A = k_0 c_A / k_{ad}^B P_B$.

With the specification above, the MC algorithm for describing the reaction is as follows.

(i) A site on the lattice is chosen at random. Then, a trial of B diffusion [item (ii)] or the catalytic cycle and A diffusion [item (iii)] is executed provided that $\rho > p$ and $\rho < p$, where ρ is a random number $(0 \leqslant \rho \leqslant 1)$.

(ii) A B-diffusion trial is performed if the site chosen is occupied by B. In this case, one of the NN sites is selected at random, and B is replaced to the latter site if it is vacant and located on the central part of the lattice.

(iii) Trials of other steps are performed, depending on the state of the site chosen. If the site is vacant and located on the central part of the lattice, it is filled by B. If the site is vacant and located on the periphery, it is filled by A with probability p_{ad}^A. If the site is occupied by B, B desorption is

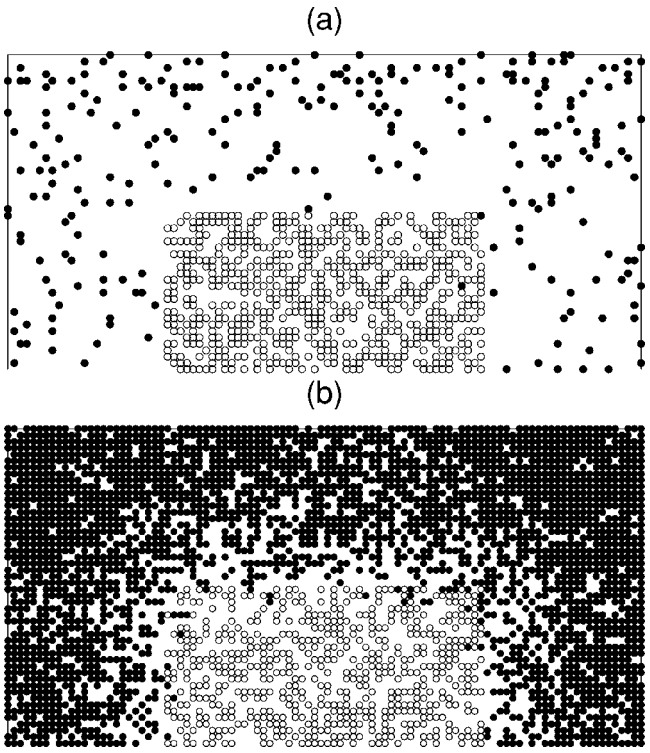

FIG. 2. Snapshots of the upper (50×100) part of the (100×100) lattice for $F=3$ (a) and 7 (b) in the case when the A binding energy on the electrolyte-metal interface is lower than on the gas-metal interface $[\exp(\Delta E/k_BT)=0.1]$. The filled and open circles represent A and B particles, respectively.

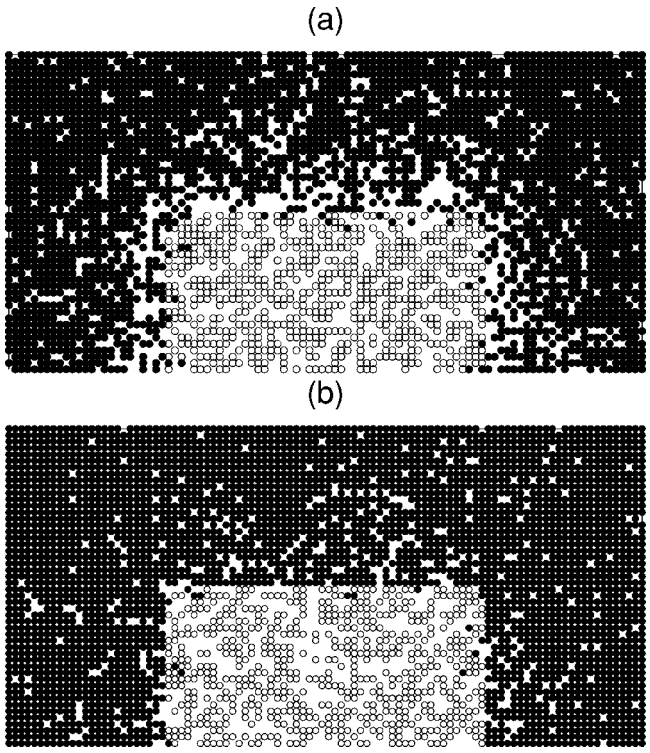

FIG. 3. Snapshots of the upper (50×100) part of the (100×100) lattice for $F=7$ in the cases when the binding energy on the electrolyte-metal is [(a) $\Delta E=0$] equal to and [(b) $\exp(\Delta E/k_BT)=10$] higher than that on the gas-metal interface. The filled and open circles represent A and B species.

realized with probability $p_{\rm des}^B$. If the site is occupied by A, one of the NN sites is selected at random, and then the $A_{\rm ads}+B_{\rm ads}$ step is realized (i.e., the reactants are removed from the lattice) with probability $p_{\rm r}$ provided that both sites are on the central part of the lattice and the latter site is occupied by B. If the latter site is vacant, the A diffusion jump is realized with probability $p_{\rm dif}^A$ provided that the A binding energy on the former site is equal to or lower than that on the latter site, or with probability $p_{\rm dif}^A\exp(-|\Delta E|/k_BT)$ provided that the binding energy on the former site is higher than on the latter site (these rules satisfy the detailed balance principle).

In MC simulations, time is calculated in MC steps (MCS). 1 MCS usually corresponds to $L\times L$ attempts to realize one of the rate processes (L is the lattice size). In our case, this definition would result in the time scale related to B diffusion, because this step is fast compared to the others. Physically, it is more convenient to relate the MC time to the time scale of the catalytic cycle. This can be done if 1 MCS is defined as $L\times L/p$ MC trials. According to this definition adopted in our simulations, the MC and real times are related as $t_{\rm MC}=k_{\rm ad}^B P_B t$, and the ECR rate calculated per one MCS is equal to that calculated per one B-adsorption trial, because we employ $p_{\rm ad}^B=1$.

To illustrate our findings, we use $p=0.01$, $p_{\rm ad}^B=1$, $p_{\rm des}^B=1$, $p_0^A=10^{-6}$, $p_{\rm r}=0.1$, and $p_{\rm dif}^A=0.5$. ΔE is chosen to equal zero or so that $\exp(|\Delta E|/k_BT)=10$. The ratio $F\equiv\alpha e_0\varphi_{\rm e}/k_BT$, employed as a governing parameter, is varied from 3 to 7. B diffusion is two orders of magnitude faster than the catalytic cycle ($p=0.01$). (In reality, the rate of B diffusion may be much faster, but increasing this rate does not change the results.)

Initially, the lattice was clean. The first 5×10^4 MCS were executed for $F=3$. This duration was sufficient in order to reach the steady state. The steady-state reaction rate was calculated during the last 10^4 MCS. Then, F was incremented by 0.5 and additional 5×10^4 MCS were performed to get a new value of the reaction rate. The latter procedure was repeated up to $F=7$.

With the parameters chosen, our model describes one of the most interesting situations when the $A_{\rm ads}+B_{\rm ads}$ reaction is fast compared to A^- adsorption and B particles are close to the adsorption-desorption equilibrium. In this case, the MF approximation predicts that (i) the A coverage is low and (ii) the reaction rate calculated per MCS is nearly equal to the rate of A^- adsorption on the bare surface, i.e., $W=\kappa(1-\kappa)^{-1}p_0^A\exp(F)$ [cf. Eq. (4)]. Our simulations indicate (Fig. 1) that these predictions are right only if F is sufficiently small. Specifically, the limits of application of the MF approximation are found to depend on ΔE. If the A binding energy on the electrolyte-metal interface is lower than or equal to that on the gas-metal interface (i.e., $\Delta E\leqslant0$), the jumps from the former interface to the latter one are energetically favorable (there is no additional Arrhenius factor for such jumps), and the MF approximation holds up to F

$\simeq 5$ (curves 1 and 2 in Fig. 1). If, however, the A binding energy on the electrolyte-metal interface is higher than that on the gas-metal interface and accordingly the jumps from the former interface to the latter one are suppressed due to the additional Arrhenius factor $[\exp(-\Delta E/k_B T)=0.1]$, the deviations from the MF approximation are appreciable already at $F=3$.

Typical lattice snapshots are shown in Figs. 2 and 3. In particular, Fig. 2 exhibits the arrangement of adsorbed particles for $F=3$ and 7 in the case when the A binding energy is lower on the electrolyte-metal interface $(\Delta E<0)$. If the electrode potential is small $(F=3)$, A^- adsorption is slow, the A coverage is low, and accordingly the ECR kinetics is close to the MF limit. If the electrode potential is appreciable $(F=7)$, A^- adsorption is still slow compared to the $A_{ads}+B_{ads}$ reaction but becomes faster than A diffusion. In the latter case, the A coverage is high and one can observe well-developed gradients in the distribution of A particles. This means that the reaction is limited by A diffusion on the peripheral part of the lattice. For $F=7$ and $\Delta E=0$, the situation is similar [cf. Figs. 2(b) and 3(a)]. If, however, $F=7$ and $\Delta E>0$, the gradients in the A distribution on the peripheral part of the lattice are weaker and simultaneously one can observe a stepwise drop in the A coverage near the line dividing the electrolyte-metal and gas-metal interfaces [Fig. 3(b)]. This indicates that the reaction is limited by A jumps via this line. With increasing lattice size, the role of this effect will increase.

In summary, we have analyzed the kinetics of the generic $A+B\rightarrow AB$ reaction occurring on metal particles with three-phase boundaries. Specifically, we have illustrated that the deviations from the Tafel law can be related to limitation of the reaction rate by diffusion of one of the adsorbed reactants along catalyst particles. In real systems, qualitatively similar deviations from the Tafel law are common [13]. Usually, this feature of ECR is attributed to the interplay between the reaction kinetics and reactant diffusion in the electrolyte or gas phase. Our results extend this concept. Potentially, our findings may be useful for applications, e.g., for optimization of the performance of fuel cells.

This work was performed in the framework of the KCK project funded by MISTRA (Grant No. 95014). The author thanks B. Kasemo for useful discussions.

[1] S. Gottesfeld and T. A. Zawodzinski, in *Advances in Electrochemical Science and Engineering*, edited by R. C. Alrice *et al.* (Wiley, Weinheim, 1997), Vol. 5, p. 195.
[2] N. M. Marcović and P. N. Ross, Surf. Sci. Rep. **45**, 117 (2002).
[3] L. Carrette *et al.*, Fuel Cells **1**, 5 (2001); M. C. Williams, *ibid.* **1**, 87 (2001).
[4] K. A. Friedrich *et al.*, Electrochim. Acta **45**, 3283 (2000); N. Chi *et al.*, Catal. Lett. **71**, 21 (2001).
[5] A. V. Petukhov, Chem. Phys. Lett. **277**, 539 (1997); M. T. M. Koper *et al.*, J. Chem. Phys. **109**, 6051 (1998); C. Korzeniewski and D. Kardash, J. Phys. Chem. B **105**, 8663 (2001); C. Saravanan *et al.*, Phys. Chem. Chem. Phys. **4**, 2660 (2002).
[6] Y. Bulten *et al.*, J. Appl. Electrochem. **29**, 1025 (1999); V. Gurau *et al.*, J. Electrochem. Soc. **147**, 2468 (2000); G. Murgia *et al.*, *ibid.* **149**, A31 (2002); F. Jaouen *et al.*, *ibid.* **149**, A437 (2002); A. A. Kulikovsky, Electrochem. Commun. **4**, 527 (2002).
[7] A. S. Ioselevich and A. A. Kornyshev, Fuel Cells **1**, 40 (2001).
[8] T. E. Springer *et al.*, J. Electrochem. Soc. **148**, A11 (2001).
[9] M. Che and C. O. Bennett, Adv. Catal. **36**, 55 (1989).
[10] V. P. Zhdanov and B. Kasemo, Surf. Sci. Rep. **39**, 25 (2000).
[11] W. Schmickler, *Interfacial Electrochemistry* (Oxford University Press, New York, 1996).
[12] A. Bogicevic *et al.*, Phys. Rev. B **57**, R4289 (1998); V. P. Zhdanov and B. Kasemo, Surf. Sci. **412**, 527 (1998).
[13] J. Ihonen *et al.*, J. Electrochem. Soc. **149**, A448 (2002).